



# Modeling phase diagrams of systems containing ionic liquids used in different applications

Yushu S. Chen, Fabrice Mutelet, Jean-Noël Jaubert

## ► To cite this version:

Yushu S. Chen, Fabrice Mutelet, Jean-Noël Jaubert. Modeling phase diagrams of systems containing ionic liquids used in different applications. 39TH EDITION OF THE JOINT EUROPEAN DAYS ON EQUILIBRIUM BETWEEN PHASES (XXXIX JEEP), Mar 2013, Nancy, France. pp.01014, 10.1051/mateconf/20130301014 . hal-01292160

**HAL Id: hal-01292160**

**<https://hal.univ-lorraine.fr/hal-01292160>**

Submitted on 13 Dec 2016

**HAL** is a multi-disciplinary open access archive for the deposit and dissemination of scientific research documents, whether they are published or not. The documents may come from teaching and research institutions in France or abroad, or from public or private research centers.

L'archive ouverte pluridisciplinaire **HAL**, est destinée au dépôt et à la diffusion de documents scientifiques de niveau recherche, publiés ou non, émanant des établissements d'enseignement et de recherche français ou étrangers, des laboratoires publics ou privés.

# Modeling phase diagrams of systems containing ionic liquids used in different applications

Y.S. Chen, F. Mutelet, and J-N. Jaubert

Laboratoire Réactions et Génie des Procédés (LRGP), Université de Lorraine, Nancy 54000, France

## 1 Introduction

Ionic liquids (ILs) [1], organic salts with melting points around or below ambient temperature, have been used as green solvents, owing to their interesting physicochemical properties: negligible vapour pressure, high chemical and thermal stabilities, and recyclability. Moreover, they are able to dissolve a wide range of organic or inorganic substances, and it is possible to adjust some of their properties such as polarity or miscibility by employing different cation-anion combinations [2-6]. For all these reasons, ILs are being postulated as promising alternative solvents for a number of technological applications in the context of green processes such as the absorption of carbon dioxide and the extractive desulfurization of diesel oil.

Thermodynamic properties of ILs can be obtained by experimental techniques and/or simulations. The main advantage of the use of an equation of state versus the other techniques is the speed and efficiency in which these calculations are performed. An equation of state such as PC-SAFT (Perturbed Chain-Statistical Associating Fluid Theory) [7] based on statistical mechanics offers several advantages. The first advantage is that each of the approximations made in the development of SAFT such as the chain and association terms has been verified from molecular simulation results. In this way, the range of applicability and the shortcomings of each term in the equation of state have been assessed. Moreover, the SAFT parameters have a physical meaning. The PC-SAFT is a useful tool in which the effects of molecular structure on the thermodynamic properties can be separated and quantified. For example, non-ideal contributions such as chain length and/or molecular shape, molecular association and polar interactions can be introduced in the development of the equation.

In this work, we present the application of the PC-SAFT equation of state to model phase diagrams of systems containing ILs. The first part of this work consists on an experimental section including vapor-liquid equilibrium (VLE) measurement for binary systems containing {ILs+CO<sub>2</sub>} and {ILs+ pyridine}. In a second part, the experimental data were correlated with

the PC-SAFT model and accurate prediction was obtained for the two binary systems.

## 2 Experimental

### 2.1 Materials

Carbon dioxide was purchased from Messer with a purity of 0.99 in mass fraction. The ILs studied in this work: 1, 3-dimethylimidazolium methylphosphonate [DMIM][Ph] (purity>98%) was obtained from Solvionic, 1-ethyl-3-methylimidazolium thiocyanate [EMIM][SCN] (purity>95%) was supplied by Fluka, trihexyl(tetradecyl)phosphonium dodecylbenzenesulfonate [THTDP][C<sub>12</sub>H<sub>25</sub>PhSO<sub>3</sub>] (purity>98%) and 1-butyl-3-methylimidazolium diethylene-glycolmonomethylethersulfate [BMIM] [MDEGSO<sub>4</sub>] (purity>98%) were supplied by STREM Chemicals Inc..

### 2.2 Apparatus and Procedure

#### VLE measurements for {CO<sub>2</sub> + ILs}

Bubble point pressures of the systems {CO<sub>2</sub> + IL} were measured using a high-pressure variable-volume visual cell (Top Industry, S.A.) shown in Figure 1. The technique used to carry out phase equilibrium measurements was based on a synthetic method which avoids sampling and analyses of the phases.

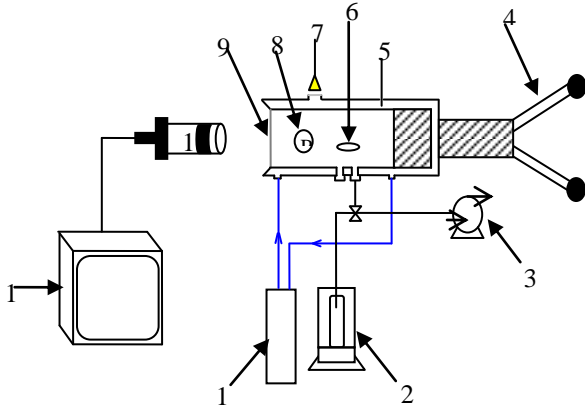


**Figure 1.** Schema of the VLE apparatus. 1: Thermostated Bath; 2: Analytical Balance; 3: Vacuum Pump; 4: Piston; 5: Temperature Probe (Pt100); 6: Magnetic stirrer; 7: Light source; 8: Calibrated pressure sensor ( $0 < P < 340\text{bar}$ ); 9: Sapphire window; 10: Video camera; 11: Monitor.

### VLE measurements for {pyridine + ILs}

VLE measurements of {pyridine + ILs} have been performed in a glass cell by using a static method. The apparatus is shown schematically in Figure 2. This apparatus can be applied for the measurement of reliable isothermal P-x data up to 298 K and 40 kPa.

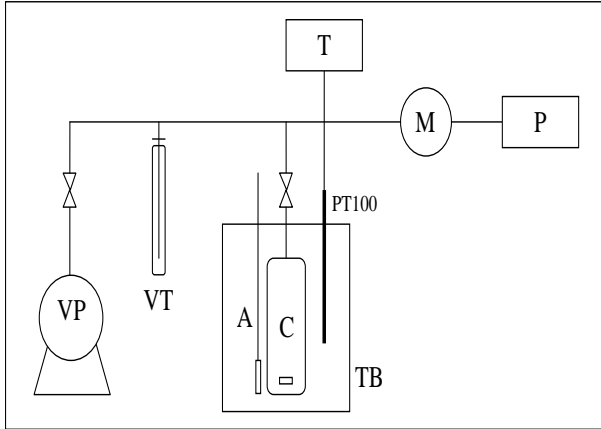


**Figure 2.** Schema of the VLE apparatus: VP: Vacuum Pump; VT: Vacuum Trap; A: Magnetic stirrer; C: Equilibrium Cell; PT-100: Platinum resistance Thermometer; T: Temperature Indicator, M: Calibrated Pressure Sensor, P: Digital Pressure Indicator and TB: Thermostated Bath.

### 3 Modeling

The Perturbed Chain-Statistical Associating Fluid Theory (PC-SAFT) EoS has been developed in 2001 by Gross and Sadowski [7]. The PC-SAFT equation is usually written in terms of the residual Helmholtz energy. Each term in the equation represents different microscopic contributions to the total free energy of the fluid. The equation writes:

$$\tilde{a}^{res} = \tilde{a}^{hc} + \tilde{a}^{disp} + \tilde{a}^{assoc} \quad (1)$$

where  $\tilde{a}^{res}$  is the residual Helmholtz free energy of the system. The superscripts *hc*, *disp* and *assoc* refer to a reference hard chain contribution, a dispersion contribution and an associating contribution, respectively. Equations are as follows:

$$\tilde{a}^{hc} = \bar{m}\tilde{a}^{hs} - \sum_{i=1}^{n_c} x_i m_i - 1 \ln g_{ij}^{hs} \quad (2)$$

$$\tilde{a}^{disp} = -2\pi\tilde{\rho}I_1\bar{m}^2\varepsilon\sigma^3 - \pi\tilde{\rho}\bar{m}C_1I_2\bar{m}^2\varepsilon^2\sigma^3 \quad (3)$$

$$\tilde{a}^{assoc} = \sum_{i=1}^{n_c} x_i \left[ \sum_{A_i} \left( \ln X^{A_i} - \frac{X^{A_i}}{2} \right) + \frac{1}{2} M_i \right] \quad (4)$$

For evaluating the phase behaviour of the {CO<sub>2</sub> + ILs} and {pyridine + ILs} systems, five parameters: the segment number (*m*), the segment energy ( $\varepsilon/k_B$ ), the segment diameter ( $\sigma$ ), the association energy ( $\varepsilon^{A_iB_j}$ ) and the association volume ( $k^{A_iB_j}$ ) are required to characterize each compound. More details about PC-SAFT equation of state have been described in our previous publication [8].

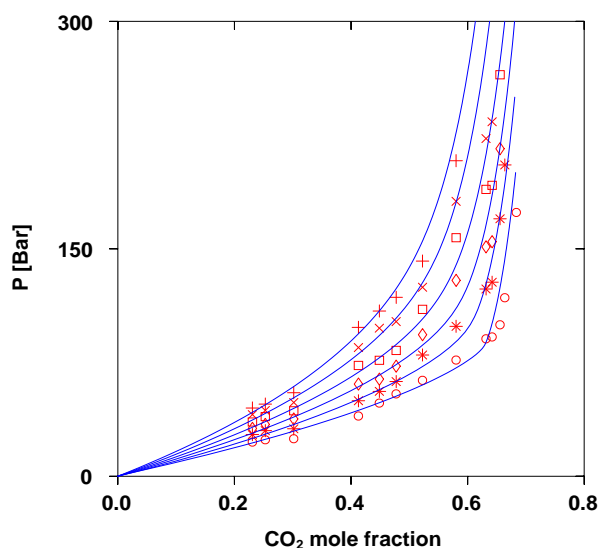
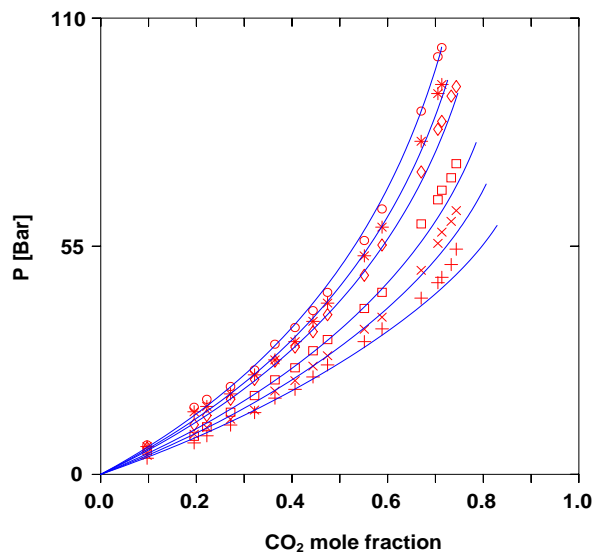
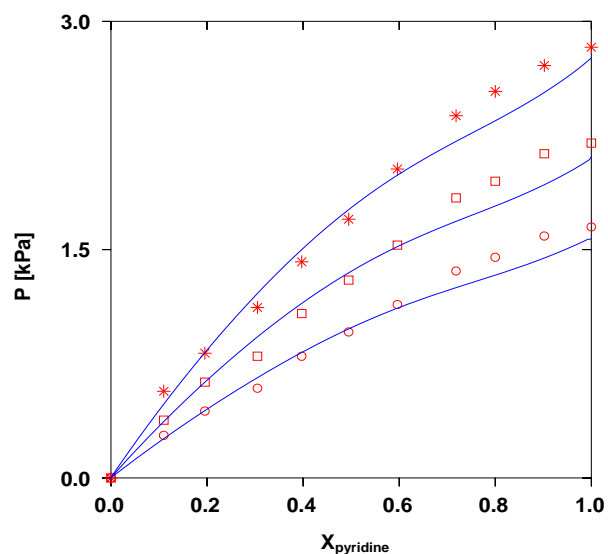
### 4 Results

The PC-SAFT parameters of pure ILs were determined using experimental densities measured in our laboratory. Carbon dioxide was modelled as a non-associating substance and represented by three molecular parameters: *m*,  $\sigma$  and  $\varepsilon/k_B$ . The values of these three parameters are taken from the literature [9]. The PC-SAFT parameters of pure ILs were determined considering them as self-associating compounds. The three non-associating parameters (*m*,  $\sigma$ ,  $\varepsilon/k_B$ ) and two self-associating parameters ( $\varepsilon^{A_iB_j}$  and  $k^{A_iB_j}$ ) were obtained by a fitting procedure on pure-component data. Parameters of pyridine were obtained from literature [10]. Results for molecular parameters of carbon dioxide, ILs and pyridine with absolute average deviation (AAD %) on density are provided in Table 1.

We now present and discuss calculations performed with the PC-SAFT EoS to correlate VLE data on systems containing {CO<sub>2</sub> or Pyridine + IL}. Interaction parameter  $k_{ij}$  was fitted on experimental VLE data. Firstly, we studied the mixture {[BMIM][MDEGSO<sub>4</sub>] + CO<sub>2</sub>} at different temperatures: T=313.15K, T=323.15K, T=333.15K, T=343.15K, T=353.15K and T=363.15K. Figure 3 depicts the experimental data but also the calculated phase diagrams using the PC-SAFT equation of state. It's striking to see the accuracy of these calculations as compared to the experimental data. Results obtained on the binary mixture {CO<sub>2</sub> + [THTDP][C<sub>12</sub>H<sub>25</sub>PhSO<sub>3</sub>]} are presented in Figure 4. A good agreement between experimental VLE data and the calculated values is observed.

**Table 1.** PC-SAFT parameters of different compounds.

	Mw (g/mol)	$\sigma$	$\varepsilon/\kappa_B$ (K)	m (-)	$\kappa_{HB}$ (-)	$\varepsilon_{HB}/\kappa_B$ (K)	AAD%
[EMIM][SCN]	169.25	4.22	383.8	3.05	0.00225	3450	0.32
[DMIM][Ph]	192.15	4.13	411.4	3.42	0.00225	3450	0.12
[BMIM][MDEGSO <sub>4</sub> ]	338.45	4.28	319.6	5.48	0.00225	3450	0.08
[THTDP][C <sub>12</sub> H <sub>25</sub> PhSO <sub>3</sub> ]	809.34	4.51	342.8	14.6	0.00225	3450	0.11
Pyridine	79.10	3.81	250.6	2.04	0.18933	1890.3	
Thiophene	84.14	3.57	301.7	2.36	0	0	
CO <sub>2</sub>	44.01	2.79	169.2	2.07	0	0	

**Figure 3.** Solubility of CO<sub>2</sub> in the [BMIM][MDEGSO<sub>4</sub>] at different temperatures: T=313K (○), T=323K (\*), T=333K (◇), T=343K (□), T=353K (×) and T=363K (+) with a temperature-dependent  $k_{ij}$  parameter. Solid lines are the PC-SAFT calculations.**Figure 4.** Solubility of CO<sub>2</sub> in the [THTDP][C<sub>12</sub>H<sub>25</sub>PhSO<sub>3</sub>] at different temperatures: T=303.15K (+), T=313.15K (×), T=323.15K (□), T=343.15K (◇), T=353.15K (\*) and T=363.15K (○) with a temperature-dependent  $k_{ij}$  parameter. Solid lines are the PC-SAFT calculations.**Figure 5.** Experimental VLE data for the investigated binary systems {Pyridine + [EMIM][SCN]} at different temperatures: T=288.15 K (○), T=293.15 K (□) and T=298.15 (\*). Solid lines are the PC-SAFT calculations.

Secondly, we studied {Pyridine + ILs} at different temperatures: T=283.15K, T=288.15K, T=293.15K and T=298.15K. As shown in Figure 5, a good agreement between experimental VLE data and the calculated phase diagrams using the PC-SAFT is observed for the system of {Pyridine + [EMIM][SCN]}. Vapor-liquid and vapor-liquid-liquid equilibrium are observed for the binary system {Pyridine + [DMIM][Ph]} (see Figure 6). The existence of one or the other depends on the concentration of mixture. Through Figure 6, it was noticeable that the phenomenon of vapor-liquid-liquid equilibrium appears from 0.51 mole fraction of pyridine at 288.15 K and the area of VLLE decreases with the increment of temperature. Furthermore, other phase

diagrams of systems such as {thiophene + ILs}, {toluene + ILs} and {water + ILs} that mainly exist in the extractive desulfurization process can be well represented by the PC-SAFT EoS.

10.D. Van Niekerk, F. Castro-Marciano, C.M. Colina, J.P. Mathews, *Energy Fuels* **25** 2559 (2011)

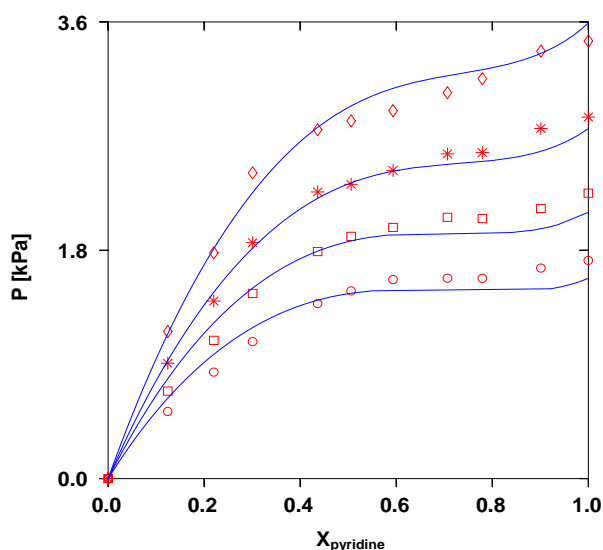


**Figure 6.** Experimental VLE data for the investigated binary systems {Pyridine + [DMIM][Ph]} at different temperatures:  $T=288.15\text{ K}$  ( $\circ$ ),  $T=293.15\text{ K}$  ( $\square$ ),  $T=298.15\text{ K}$  ( $*$ ) and  $T=303.15\text{ K}$  ( $\diamond$ ). Solid lines are the PC-SAFT calculations.

## 5 Conclusion

Phase diagrams of systems containing {ILs+CO<sub>2</sub>} and {ILs+ pyridine} were studied in a wide range of temperatures and pressures. It was found that ILs may have a good capacity for CO<sub>2</sub> absorption and fuels desulfurization. A thermodynamic model based on the PC-SAFT EoS was used with success in the correlation of the measured VLE data. The model provides a good description of phase diagrams of these mixtures.

## References

1. M.J. Earle, K.R. Seddon, *Green Chem.* **72** 1391 (2000)
2. A.L. Revelli, F. Mutelet, J.-N. Jaubert, *Ind. Eng. Chem. Res.* **49** 3883 (2010)
3. F. Mutelet, A.L. Revelli, J.-N. Jaubert, L.M. Sprunger, W.E. Acree, G.A. Baker, *J. Chem. Eng. Data* **55** 234 (2010)
4. F. Mutelet, J.-N. Jaubert, M. Rogalski, J. Harmand, M. Sindt, J.L. Mieloszynski, *J. Phys. Chem. B* **112** 3773 (2008)
5. A.L. Revelli, F. Mutelet, M. Turmine, R. Solimando, J.-N. Jaubert, *J. Chem. Eng. Data* **54** 90 (2009)
6. A.L. Revelli, F. Mutelet, J.-N. Jaubert, *J. Chromatogr. A* **1216** 4775 (2009)
7. J. Gross, G. Sadowski, *Ind. Eng. Chem. Res.* **40** 1244 (2001)
8. Y.S. Chen, F. Mutelet, J.-N. Jaubert, *J. Phys. Chem. B* **116** 14375 (2012)
9. S.H. Huang, M. Radosz, *Ind. Eng. Chem. Res.* **29** 2284 (1990)